

Angle-resolved photoemission and first-principles electronic structure of single-crystalline α -uranium (001)

C.P. Opeil

*Department of Physics, Boston College, Chestnut Hill, MA 02467, USA and
Materials Science and Technology Division, Los Alamos National Laboratory, Los Alamos, NM 87545*

R.K. Schulze, H.M. Volz, J.C. Lashley, M.E. Manley, W.L. Hulst, R.J. Hanrahan Jr., and J.L. Smith

Materials Science and Technology Division, Los Alamos National Laboratory, Los Alamos, NM 87545

B. Mihaila

*Materials Science and Technology Division, Los Alamos National Laboratory, Los Alamos, NM 87545 and
Theoretical Division, Los Alamos National Laboratory, Los Alamos, NM 87545*

K.B. Blagoev and R.C. Albers

Theoretical Division, Los Alamos National Laboratory, Los Alamos, NM 87545

P.B. Littlewood

Cavendish Laboratory, J.J. Thomson Avenue, Cambridge CB3 0HE, United Kingdom

Continuing the photoemission study begun with the work of Opeil *et al.* [Phys. Rev. B **73**, 165109 (2006)], in this paper we report results of an angle-resolved photoemission spectroscopy (ARPES) study performed on a high-quality single-crystal α -uranium at 173 K. The absence of surface-reconstruction effects is verified using X-ray Laue and low-energy electron diffraction (LEED) patterns. We compare the ARPES intensity map with first-principles band structure calculations using a generalized gradient approximation (GGA) and we find good correlations with the calculated dispersion of the electronic bands.

PACS numbers: 79.60.-i, 71.20.Gj, 71.27.+a

I. INTRODUCTION

To understand the effects of electronic correlations is one of the principal challenges in the theory of metals^{1,2}, and the actinide elements in the periodic table allow systematic exploration of the role of electron correlation effects. With increasing atomic number the f-orbitals shrink, so that Coulomb interactions become increasingly dominant along the series beginning with Th. The eventual dominance of the Coulomb repulsion over the electronic kinetic energy produces a transition between the itinerant metallic states of the early actinides and the predominantly localized f-states of the later actinides, beyond Pu. As well as a strong reorganization of the electronic structure near the transition, a characteristic feature of this regime is strong electron-lattice coupling as the different electronic configurations cause complex crystal structures.

Uranium lies close to the boundary but with predominantly itinerant character, and as the heaviest natural element is fundamental to the study of nuclear and heavy-fermion physics³. In the α phase (i.e. the crystal structure of uranium below 935 K), uranium undergoes a series of low-temperature instabilities that are thought to arise from strong electron-phonon coupling present in α -U. This coupling is also responsible for other unusual physical properties, such as the anisotropic thermal expansion⁴ and the strong temperature dependence

of the elastic moduli⁵. Recently, it was reported that the phonon spectrum of α -U exhibits an unusually large thermal softening of the phonon frequencies, suggesting that thermal effects on the electronic structure in α -U are more significant thermodynamically than classical volume effects⁶. Furthermore, interest in the study of α -U properties has been stimulated by the advent of a generation of high-quality α -U single crystals (see Refs.^{7,8} for details regarding the preparation and purity of these

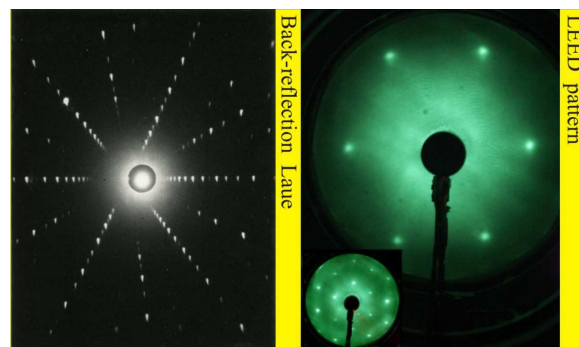


FIG. 1: LEED patterns at two energies (75 and 150 eV, respectively, the latter referring to the inset) and X-ray Laue diffraction pattern from the (001) α -U single crystal at room temperature. The LEED and Laue patterns characterize the long-range atomic order of the crystal on two different spatial scales.

crystals). Owing to their superior properties, these α -U single crystals have been the subject of many recent investigations^{8,9,10,11,12,13}.

II. ANGLE-RESOLVED PHOTOEMISSION OF A (001) α -URANIUM SINGLE CRYSTAL

Photoemission spectroscopy has the ability to probe in detail the electron-energy dispersions in the solid and band structure mapping through angle-resolved photoemission spectroscopy (ARPES) offers an ideal testbed for *ab initio* theoretical approaches to ground-state properties and electronic correlations in metals. Past experiments on U^{14,15,16,17} have suffered from ambiguity caused by measurements made on poorly defined or characterized surfaces, caused by either contaminations issues or possible formation of phases incompatible with any of the known bulk phases of uranium metal (orthorhombic α , tetragonal β , and *bcc* γ phases) in the case of U thin-film formation¹⁶. Uncertainties related to the chemical interaction between the overlayer and the substrate in thin-film deposition studies, for example, make difficult the direct comparison between theory and experiment. Using large α -U samples and a thorough sputter-anneal regimen we have overcome these difficulties. In this paper, we report high-resolution ARPES data on high-quality α -U single-crystals at 173 K.

Ultraviolet photoelectron spectra were recorded with a resolution of 28.5 meV using a Perkin-Elmer/Physical Electronics Model 5600 ESCA system equipped with a monochromated Al $K\alpha$ (1486.6 eV) XPS source, a SPECS UVS 300 ultraviolet lamp (HeI, $h\nu=21.2$ eV), and a spherical capacitor analyzer. The vacuum chamber, which had a base pressure of 10^{-12} torr, was equipped with a variable temperature sample stage of the range 150–1273 K. Prior to the ARPES experiments, the surface preparation consisted of repeated cycles of Ar ion sputtering and annealing at 873 K. As temperature is reduced to 673 K, the surface reorders, and a low-energy electron diffraction (LEED) pattern appears, see Fig. 1. Major contaminant indicators, oxygen (O1s) and carbon (C1s) signals in the XPS spectra were below the detection limit (< 1 at. %) ¹⁸. Surface cleanliness was carefully examined to insure that all features in the ARPES are due to the intrinsic α -U surface and not surface contamination. To assure that the ARPES results reflect the bulk properties of α -U, we used X-ray diffraction and LEED to study the structure of the surface at room temperature. As shown in Fig. 1, our data found no detectable structural distortions and show that the *c* axis is perpendicular to the platelet surface (see Brillouin zone depicted in Fig. 2).

The crystal surface is aligned perpendicular to the analyzer, which is set at an acceptance angle of ± 2 degrees to optimize the instrumental sensitivity. We choose a particular azimuthal angle ϕ in order to specify the direction to be probed in the (001) plane. We also vary the

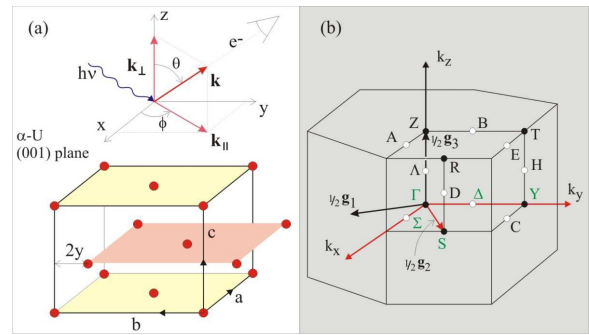


FIG. 2: (a) Schematic of the photoemission experiment relative to the single-crystal orientation²⁴. (b) Brillouin zone corresponding to the α -U single crystal (see Fig. 3.6b in Ref.²⁷). Here, \mathbf{g}_i indicate the reciprocal lattice vectors, $\mathbf{g}_1 = 2\pi/(ba)(b, -a, 0)$, $\mathbf{g}_2 = 2\pi/(ba)(b, a, 0)$, $\mathbf{g}_3 = 2\pi/c(0, 0, 1)$.

polar angle θ to specify the components of the *in-plane* momentum component, $k_{||}$, as illustrated in Fig. 2a. The polar angle was varied in steps of 1° between 0° (normal emission) and 30° , and in steps of 5° between 30° and 60° , with an estimated angular error of $\pm 0.5^\circ$. The energy-distribution curve has been measured at each electron emission angle. Three sets of data were obtained for the azimuthal angles corresponding to $\tilde{\Gamma}\tilde{\Sigma}$, $\tilde{\Gamma}\tilde{\Delta}$, and $\tilde{\Gamma}\tilde{S}$ directions²⁵ in the (001) plane (see Fig. 2b²⁷).

In contrast with our previous photoemission study in which we have investigated only photoemission ($\theta = 0$) along the $\tilde{\Gamma}$ direction¹⁸, in this work we have not attempted to carry out ARPES measurements for both HeI and HeII energy excitations. It is true that, because of cross section effects, the atomic photoionization energies at HeI and HeII energies are such that the HeII spectra are more sensitive to *f*-electron physics, whereas any *d*-electron feature will be enhanced in the HeI spectra. However, the electronic mean-free path is probably close to its minimum value for the HeII spectra, and hence any surface state will be enhanced relative to bulk states for the HeII spectra. Therefore, we have opted for performing only HeI measurements. This is also the photoionization energy for which the resolution of our experimental setup is optimal.

III. FIRST-PRINCIPLES ELECTRONIC STRUCTURE CALCULATIONS USING THE GGA/FLAPW METHOD

The photoemission data are compared with results of first-principles band-structure calculations performed using the generalized gradient approximation approach (GGA)¹⁹ in the full-potential linearized-augmented-plane-wave (FLAPW) method²⁰, with added local orbitals for a better variational flexibility in the radial basis functions²¹. The core states are treated fully relativistically, whereas the valence *d* and *f* states relativistic effects are implemented using a second-order variational

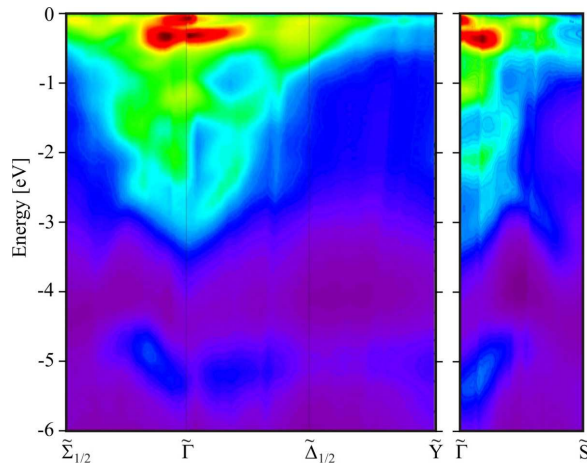


FIG. 3: Intensity map of the ARPES spectrum from the (001) α -U single crystal. Here, the color scale runs between violet (low intensity) and red (high intensity). The symbols $\tilde{\Sigma}_\alpha$ and $\tilde{\Delta}_\alpha$ indicate the symmetry lines $(\alpha, \alpha, 0)$ and $(-\alpha, \alpha, 0)$ depicted in Fig. 2. See also Ref.²⁵.

method including spin-orbit coupling²², and using the scalar-relativistic orbitals as basis. Our band structure results are consistent with previous first-principles calculations of properties of uranium metal via the full potential version of the linear muffin-tin orbital (FP-LMTO) method²³. The GGA/FLAPW approach was shown recently to compare favorably with the X-ray photoemission spectroscopic (XPS) measurements on the same single crystal of α -U at room temperature¹⁸ and reproduces the spin-orbit splitting of the 6p core levels in α -U. The ground-state structure for α -uranium is the orthorhombic space group $Cmcm$ (no. 63), with uranium atoms located at the 4c positions: $(0, y, \frac{1}{4})$ and $(0, -y, \frac{3}{4})$ plus C-centering. In our calculations, we have used the experimental lattice parameters $a=2.858$ Å, $b=5.876$ Å, $c=4.955$ Å, and $y=0.105$ ²⁴. This structure is shown in Fig. 2a, where for clarity we have translated the origin of the unit cell to coincide with an atom position.

IV. RESULTS AND DISCUSSIONS

In an ARPES experiment, the binding energy and crystal momentum of the electron in the solid are related to the frequency of the incident photon via the total energy and momentum conservation laws, i.e.

$$E_{\mathbf{KE}} = h\nu - \Phi - |E_{\mathbf{b}}|, \quad (1)$$

$$k_{\parallel} = \sqrt{(2m/\hbar^2) E_{\mathbf{KE}}} \sin \theta, \quad (2)$$

where Φ is the *work function* of the spectrometer. These two equations, valid in the noninteracting-electron approximation, constrain only the electron kinetic energy $E_{\mathbf{KE}}$ and the *in-plane* component of the electron momentum, \mathbf{k}_{\parallel} , whereas the value of the electron momentum

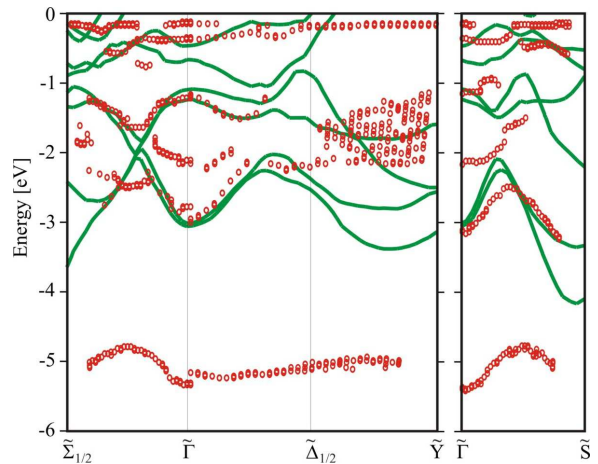


FIG. 4: Positions of the local maxima in the ARPES intensity map, together with the corresponding calculated band structure. Assuming a free-electron final-state model, the value of k_{\perp} was obtained using a zero inner-potential value, V_0 (see the discussion in Ref.²⁵ for further details).

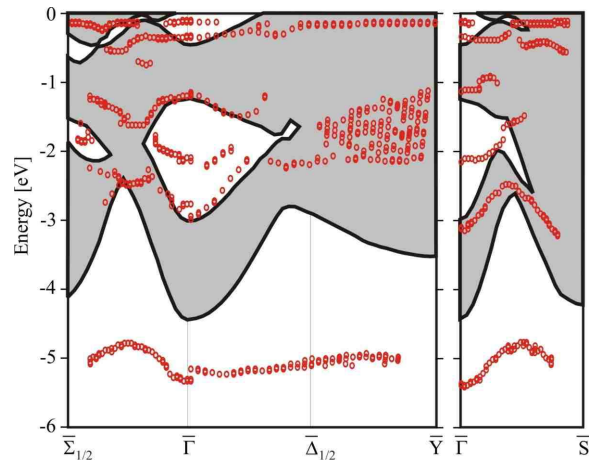


FIG. 5: Positions of the local maxima in the ARPES intensity map, together with the projection of the α -U bulk-derived bands onto the (001) surface Brillouin zone. The shaded regions indicate the range of values where α -U energy bands exist when projected onto the $\bar{\Gamma}$ to $\bar{\Sigma}$, $\bar{\Gamma}$ to $\bar{\Delta}$, and $\bar{\Gamma}$ to \bar{S} directions. The white areas indicate the gaps in the bulk electronic band structure in which a surface state might exist.

perpendicular to the sample surface, k_{\perp} , is not well defined because of the termination of the translational symmetry normal to the sample surface. The uncertainty of k_{\perp} is expected to be $\sim 0.2 \div 0.3$ Å⁻¹ for a photon energy $h\nu \sim 20$ eV on the basis of the mean-free path of electron in solids, $\sim 3 \div 5$ Å, which is significantly smaller than the wave-vector along the c axis of α -U, $2\pi/c \sim 1.2$ Å⁻¹, and can be neglected. Then, the intensity measured in the ARPES experiment, $I(\mathbf{k}_{\parallel}, \omega)$, is proportional to the electronic density of states, weighed by the square of the transition matrix element, $|M_{fi}^{\mathbf{k}}|^2$, of the photon-electron

interaction between the initial and final states of the N-particle system, i.e.

$$I(\mathbf{k}_{\parallel}, \omega) \propto |M_{fi}^{\mathbf{k}}(\nu, \hat{\epsilon})|^2 N(\mathbf{k}, \omega) f(\omega), \quad (3)$$

where $|M_{fi}^{\mathbf{k}}(\nu, \hat{\epsilon})|^2$ depends on the electron momentum and on the energy ($h\nu$) and polarization ($\hat{\epsilon}$) of the incident photon. $N(\mathbf{k}, \omega)$ is the electron directional-dependent density of states of the electron, and the Fermi function, $f(\omega) = (e^{\hbar\omega/k_B T} + 1)^{-1}$, is included in Eq. (3) because photoemission spectroscopy probes only the occupied electronic states. While a quantitative analysis of the ARPES experimental results, requiring the detailed modeling of the structure function, is beyond the scope of this study, we find interesting correlations between the experimental intensity map, $I(\mathbf{k}_{\parallel}, \omega)$, and bulk electronic band structure calculated using the GGA/FLAPW method.

Figure 3 shows the α -U single-crystal ARPES data at HeI photon energy as a function of the component of the electron momentum in the (001) plane, k_{\parallel} . For comparison, in Fig. 4 we plot the positions of the intensity maxima in the ARPES intensity map together with the corresponding electronic band structure. We observe good correlations between the ARPES and the calculated band structure, which tracks the main features of the photoemission landscape in the (001) plane. However, the high-intensity spectral structures located close to the Fermi surface are shifted with respect to the high-density level regions in the band structure. We also notice several features which do not have a correspondent in the calculated bulk electronic band structure. In particular, we confirm the presence of peaks located at -0.1 eV, -2.2 eV along the Γ direction (see also Ref.¹⁸).

For a photon at the HeI energy, $h\nu=21.2$ eV, the plot of the “universal” escape depth (see chapter 1 in Ref.²⁶) indicates the escape depth in our experiment is less than 10 Å, which must be compared with the lattice spacing in the c direction ($c=4.955$ Å). Therefore, in an ARPES experiment at this photon energy, we probe at most 2-3 atomic layers perpendicular to the (001) surface, and surface scattering may contribute to the measured photoemission spectrum. While the dirt contributions due to surface states have been minimized through careful surface preparation¹⁸, we may still observe the presence of surface states located in the gaps of the bulk band structure (see chapter 8 in Ref.²⁶ and Refs.^{28,29}). The shaded region shown in Fig. 5 indicates the range of values where α -U energy bands exist when projected onto the (001) plane. The white areas indicate possible regions where surface states might exist.

The GGA/FLAPW approximation used here, captures part of the electronic correlations, but is not able to describe the strongly-varying electronic density in heavy-

fermion materials². Therefore, the discrepancies between our calculations and the observed ARPES spectra can be attributed in part to the strong correlations in the electronic liquid or yet unidentified contribution of surface or collective states. A recent analysis of the specific-heat data below 10 K, measured on α -U samples of the same pedigree⁸, gives an electronic specific heat $\gamma_{\text{exp}}=9.13$ mJ K⁻² mol⁻¹ and a low-temperature limiting Debye temperature $\Theta_D=256$ K. Using these values, and taking the band structure $\gamma_{\text{b.s.}}=5.89$ mJ K⁻² mol⁻¹, we obtain an upper bound on the mass-enhancement factor³⁰, $m^*/m_{\text{b.s.}} = \gamma_{\text{exp}}/\gamma_{\text{b.s.}} = 1.55$, for α -U single crystal. This modest fermi edge mass enhancement could of course have its origin in either or both of the electron-phonon coupling or electron correlation effects, which go beyond those included in the GGA/FLAPW band-structure calculations. If the former, the redistribution of spectral weight will disappear rapidly off-shell, whereas the electron-electron interactions would play an increasing role at higher energies. The generally good correlations between experiment and theory suggest that correlations effects are not very large in α -U, and that it is appropriate to think of it as a band metal, and not a highly-correlated system.

V. CONCLUDING REMARKS

In summary, in this paper we report high-resolution ARPES measurements of a high-quality (001) α -U single crystal and compare them with first-principles electronic band structure calculations using the GGA/FLAPW method. Together with detailed theoretical studies of electronic correlation effects, further photoemission studies at a synchrotron radiation source (necessary to take advantage of an improved energy resolution and the ability to modify the incident photon energy) are being pursued in order to understand quantitatively the band structure using ARPES in α -U single crystals.

Acknowledgments

This work was supported in part by the LDRD program at Los Alamos National Laboratory. B.M. acknowledges financial support from ICAM. The authors gratefully acknowledge the contribution of the U(001) samples from: H.F. McFarlane, K.M. Goff, F.S. Felicione, C.C. Dwight, D.B. Barber, C.C. McPheeters, E.C. Gay, E.J. Karell and J.P. Ackerman at Argonne National Laboratory. B.M. would like to thank D.L. Smith, J.M. Wills, M.D. Jones, and I. Schnell for useful discussions.

¹ A.A. Abrikosov, *Fundamentals of the Theory of Metals*, (North-Holland, Amsterdam, 1988).

² P. Fulde, *Electron Correlations in Molecules and Solids*,

- (Springer-Verlag, Berlin, 1995).
- ³ G.H. Lander, E.S. Fisher, and S.D. Bader, *Adv. Phys.* **43**, 1 (1994).
 - ⁴ L.T. Lloyd and C.S. Barrett, *J. Nucl. Mater.* **18**, 55 (1966).
 - ⁵ E.S. Fisher and H.J. McSkimin, *Phys. Rev.* **124**, 67 (1961); E.S. Fisher, *J. Nucl. Mater.* **18**, 39 (1966).
 - ⁶ M.E. Manley, B. Fultz, R.J. McQueeney, C.M. Brown, W.L. Hulth, J.L. Smith, D.J. Thoma, R. Osborn, and J.L. Robertson, *Phys. Rev. Lett.* **86**, 3076 (2001).
 - ⁷ H. F. McFarlane, K.M. Goff, F.S. Felicione, C.C. Dwight and D.B. Barber, *JOM* **49**, 14 (1997); C. C. McPheeters, E.C. Gay, P.J. Karell, and J. Ackerman, *JOM* **49**, 22 (1997).
 - ⁸ J.C. Lashley, B.E. Lang, J. Boerio-Goates, B.F. Woodfield, G.M. Schmiedeshoff, E.C. Gay, C.C. McPheeters, D.J. Thoma, W.L. Hulth, J.C. Cooley, R.J. Hanrahan, and J.L. Smith, *Phys. Rev. B* **63**, 224510 (2001).
 - ⁹ M.E. Manley, G.H. Lander, H. Sinn, A. Alatas, W. L. Hulth, R. J. McQueeney, J. L. Smith, and J. Willit, *Phys. Rev. B* **67**, 052302 (2003).
 - ¹⁰ G.M. Schmiedeshoff, D. Dulguerova, J. Quan, S. Touton, C.H. Mielke, A.D. Christianson, A.H. Lacerda, E. Palm, S.T. Hannahs, T. Murphy, E.C. Gay, C.C. McPheeters, D.J. Thoma, W.L. Hulth, J.C. Cooley, A.M. Kelly, R.J. Hanrahan, and J. L. Smith, *Phil. Mag.* **84**, 2001 (2004).
 - ¹¹ E.J. Nelson, P.G. Allen, K.J.M. Blobaum, M.A. Wall and C.H. Booth, *Phys. Rev. B* **71**, 184113 (2005).
 - ¹² B. Mihaila, C.P. Opeil, F.R. Drymiotis, J.L. Smith, J.C. Cooley, M.E. Manley, A. Migliori, C. Mielke, T. Lookman, A. Saxena, A.R. Bishop, K.B. Blagoev, D.J. Thoma, and J.C. Lashley, B.E. Lang, J. Boerio-Goates, B.F. Woodfield, and G.M. Schmiedeshoff, *Phys. Rev. Lett.* **96**, 076401 (2006).
 - ¹³ M.E. Manley, M. Yethiraj, H. Sinn, H.M. Volz, A. Alatas, J.C. Lashley, W.L. Hulth, G.H. Lander, and J.L. Smith, *Phys. Rev. Lett.* **96**, 125501 (2006).
 - ¹⁴ W.D. Schneider and C. Laubschat, *Phys. Rev. B* **23**, 997 (1981).
 - ¹⁵ T.H. Gouder and C.A. Colmenares, *Surf. Sci.* **341**, 51 (1995).
 - ¹⁶ S.L. Molodtsov, J. Boysen, M. Richter, P. Segovia, C. Laubschat, S.A. Gorovikov, A.M. Ionov, G.V. Prudnikova, and V.K. Adamchuk, *Phys. Rev B* **57**, 13241 (1998).
 - ¹⁷ S.L. Molodtsov, S.V. Halilov, M. Richter, A. Zangwill and C. Laubschat, *Phys. Rev. Lett.* **87**, 017601 (2001).
 - ¹⁸ C.P. Opeil, R.K. Schulze, M.E. Manley, J.C. Lashley, W.L. Hulth, R.J. Hanrahan Jr., J.L. Smith, B. Mihaila, K.B. Blagoev, R.C. Albers, and P.B. Littlewood, *Phys. Rev. B* **73**, 165109 (2006).
 - ¹⁹ J.P. Perdew, K. Burke, M. Ernzerhof, *Phys. Rev. Lett.* **77**, 3865 (1996).
 - ²⁰ P. Blaha, K. Schwarz, G.K.M. Madsen, D. Kvasnicka and J. Luitz, WIEN2k, An Augmented Plane Wave Plus Local Orbitals Program for Calculating Crystal Properties (Karlheinz Schwarz, Technische Universitt Wien, Austria, 2001).
 - ²¹ J. Kunes, P. Novák, R. Schmid, P. Blaha and K. Schwarz, *Phys. Rev. B* **64**, 153102 (2001).
 - ²² A.H. MacDonald, W.E. Pickett, and D.D. Koelling, *J. Phys. C* **13**, 2675 (1980).
 - ²³ P. Söderlind, *Phys. Rev. B* **66**, 085113 (2002).
 - ²⁴ J. Akella, S. Weir, J.M. Wills and P. Söderlind, *J. Phys., Condens. Matter.* **9**, L549 (1997).
 - ²⁵ In a three-dimensional electron system such as αU , the dispersion along the k_{\perp} cannot be neglected. Therefore, we have introduced the notation $\tilde{\Gamma}$ to make it clear that the photoemission experiment does *not* simply probe the Γ point. See discussion in chapter 7 of Ref.²⁶.
 - ²⁶ S. Hüfner, *Photoelectron Spectroscopy*, 2nd ed. (Springer Verlag, New York, 1995).
 - ²⁷ In this paper we use the conventions introduced in C.J. Bradley and A.P. Cracknell, *The Mathematical Theory of Symmetry in Solids* (Clarendon Press, Oxford, 1972).
 - ²⁸ I. Tamm, *Z. Phys.* **76**, 848 (1932).
 - ²⁹ W. Shockley, *Phys. Rev.* **56**, 317 (1939).
 - ³⁰ See e.g. G. Grimvall, *The electron-phonon interaction in metals* (North-Holland Publishing Company, Amsterdam, 1981).